Preprint Accepted for publication in *Neurosci. Res.* (2024) **xxx**: xxx

Estimation of firing rate from instantaneous interspike intervals

Lubomir Kostal* and Kristyna Kovacova

Institute of Physiology of the Czech Academy of Sciences, Videnska 1083, 14200 Prague 4, Czech Republic

The rate coding hypothesis is the oldest and still one of the most accepted hypotheses of neural coding. Consequently, many approaches have been devised for the firing rate estimation, ranging from simple binning of the time axis to advanced statistical methods. Nonetheless the concept of firing rate, while informally understood, can be mathematically defined in several distinct ways. These definitions may yield mutually incompatible results unless implemented properly. Recently it has been shown that the notions of the instantaneous and the classical firing rates can be made compatible, at least in terms of their averages, by carefully discerning the time instant at which the neuronal activity is observed. In this paper we revisit the properties of instantaneous interspike intervals in order to derive several novel firing rate estimators, which are free of additional assumptions or parameters and their temporal resolution is 'locally self-adaptive'. The estimators are simple to implement and are numerically efficient even for very large sets of data.

Keywords: Spike train; Firing rate; Estimator; Big data

1. INTRODUCTION

Biological neuronal systems show impressive capabilities of learning, decision making or action coordination, by employing the information encoded from both the external and the internal environments. Despite significant effort of experimental and theoretical neuroscientists the exact quantitative mechanism of neuronal coding remains uncertain. Generally, neurons communicate by using chemical and electrical synapses. The key event that triggers synaptic transmission is the action potential (also denoted as spike), which is a pulse of electrical discharge traveling along the axonal excitable membrane. The shape (time course in time) and duration of individual spikes of any given neuron are essentially identical, therefore the whole spike train (series of spikes in time) can be described as a sequence all-or-none point events. On the other hand, the exact timing of spikes, even under identical external conditions, typically varies from trial to trial [1–3].

There are essentially two main hypotheses describing the way information is represented in spike trains [1, 4]: the *temporal* and *rate* (also denoted as frequency) coding schemes. According to the rate coding hypothesis, the intensity or strength of a stimulus is represented by the average firing rate of neurons over a certain period of time. In other words, higher firing rates correspond to stronger stimuli or increased activity in a neural circuit, while lower firing rates indicate weaker stimuli or reduced activity. The rate coding hypothesis is the oldest and still one of the most accepted and investigated scenarios in neuronal activity analyses in both theoretical and experimental works, see, e.g., Gerstner and Kistler [1], Dayan and Abbott [5], Adrian [6], Kandel *et al.* [7], Lee *et al.* [8], Kostal and Kobayashi [9], Abeles [10], Shinomoto [11], Koyama and Kostal [12] and references therein. Furthermore, the rate coding hypothesis provides a conceptual framework for understanding how populations of neurons collectively encode complex stimuli or perform computations. By combining information from multiple neurons with different tuning properties and response characteristics, neural circuits can represent a wide range of sensory inputs and perform sophisticated information processing tasks. However, it is worth noting that the key terms (firing) rate, mean rate, frequency or mean/instantaneous frequency are used differently by different authors, depending on the context [1, 13].

Elementary observation reveals that even if the firing rates are the same, the resulting spike trains can have very different appearances [4]. The question whether the temporal structure of ISIs is due to fluctuations in spike generation (e.g., neuronal noise) or whether it represents an informative part of the neuronal signal is not yet fully resolved [3, 14] and leads to the concept of temporal coding [1, 15]. The temporal coding is assumed to be the dominant coding scheme in the sustained stationary part of neuronal response [16, 17]. Generally, temporal codes employ those features of the spiking activity that cannot be described by the firing rate, in particular the individual lengths of *interspike inetrvals* (ISIs) For a classic overview of temporal coding see Perkel and Bullock [18], for a more recent discussion see Stein *et al.* [3], Abeles [10], Shadlen and Newsome [14], Rieke *et al.* [19], Theunissen and Miller [20]. It follows that any information possibly encoded in the temporal structure of the spike train is ignored in the rate coding scheme. Consequently, rate coding is inefficient but highly robust with respect to the ISI 'noise' [3, 4, 21].

Accurate neuronal firing rate estimation is therefore a crucial aspect of neuroscientific research, involving vari-

* E-mail: kostal@biomed.cas.cz

ous computational techniques and mathematical models. Traditional methods often involve binning spike times into small time intervals and counting the number of spikes within each bin to compute firing rates. However, these approaches may suffer from biases or inaccuracies, especially when dealing with sparse or irregular spike trains [11]. To address these challenges, researchers have developed advanced statistical methods and signal processing techniques, e.g., Bayesian approaches, point process models and techniques [22–26], see e.g., Tomar [27] for a recent overview.

The main goal of this paper is to introduce a novel method for firing rate estimation which differs substantially from the classical approaches mentioned above. Particularly, the reciprocal value of the interval between consecutive spikes — known as the instantaneous firing rate [28, 29] — is sometimes used as the alternative to the 'standard' firing rate. The advantage of the instantaneous rate concept lies in the fact that ISI statistics are often more easily obtainable than count-based statistics. Although the physical dimension of the instantaneous rate is compatible with the firing frequency, the two quantities generally yield incompatible results [13]. However, the recently introduced concept of *instantaneous interspike intervals* [30] statistically corrects the difference between the two notions of firing rate. Here we reconsider the instantaneous rate as the basis for firing rate estimation and we construct explicit estimators which are: *i)* sufficiently general, applicable to non-stationary situations, *ii)* computationally very simple to be readily implemented even for big datasets, *iii)* free of additional parameters that would need to be optimized over and *iv)* with locally adaptive temporal resolution (meaning that the method can be used for both low- and high-firing neuronal regimes). Furthermore, since our method is based on the reciprocal value of individual ISIs, it reduces the strict distinction between the temporal and the rate coding schemes.

The paper is organized as follows. First we briefly review the essential concepts of firing rate, instantaneous rate, the estimation methods and the Cramér-Rao bound, which allows us to evaluate the estimator efficiency. In the results section we derive both the non-parametric and the maximum likelihood estimators for few popular statistical models of neuronal activity, including for the generalized Poisson process with a refractory period. We believe the most practically useful results are represented by the explicit and algebraically simple formulas for the firing rate estimators as given by Eqs. (42), (49) and (55). Finally, we compare the new approach with state-of-art self-adaptive firing rate estimation methods [22, 23], and discuss the advantages and the limitations of tour method.

2. METHODS

2.1. Spike train as a stochastic point process

Individual spikes in a spike train are usually well separated, but their exact timing often varies, apparently randomly, both within and across trials. Conveniently, the whole spike train is formally described as a series of all-or-none point events in time – the (stochastic) point process [31–34]. In the following we briefly review the key notions of the theory which are essential for both the instantaneous and the classical firing rate definitions [30].

Assume the spike times are denoted as $0 < S_1 < S_2 < \dots$. Generally, the time origin, $t = 0$, is not related to the actual spike times, i.e., it is naturally fixed with respect to some reference value (i.e., the 'laboratory time') before the point process realization. The interspike intervals (ISIs), Y_i, are then defined as (see Fig. 1A).

$$Y_i = S_{i+1} - S_i, \quad i = 1, 2, \dots \tag{1}$$

The associated process of counts, $N(t_1, t_2)$, for any two times $t_2 > t_1$, is a random variable describing the number of spikes in some interval $(t_1, t_2]$. The spike times S_i and the process $N(0, t)$ are equivalently related by the formula

$$\{S_i \le t\} = \{N(0, t) \ge i\}, \quad i = 1, 2, \dots \tag{2}$$

The expected spike count in $(t_1, t_2]$ is denoted as $E[N(t_1, t_2)]$. The *firing intensity* $\lambda(t)$ of the spiking process at some time t is defined as the rate of change of the mean spike count at this time,

$$\lambda(t) = \lim_{\varepsilon \downarrow 0} \frac{E[N(t, t+\varepsilon)]}{\varepsilon}. \tag{3}$$

Note that the probability distribution of $N(t, t+\varepsilon)$ generally depends on the history (i.e., on the preceding spike times) of the process up to time t, hence $\lambda(t)$ is frequently called the *conditional intensity* of the point process. The history dependence can be reduced considerably for simple, e.g., renewal, ISI models (see below).

Often in experiments the limit in Eq. (3) is not available, and the firing rate is defined as the number of spikes in a sufficiently long time window, w, which is set by the experimenter. Typical values are, e.g., $w = 100\,\text{ms}$ or $w = 500\,\text{ms}$, but can be longer or shorter depending on the experimental setup and the neuron recorded [1, Ch. 1.5]. The (mean) firing rate ν is defined as [5, 6],

$$\nu(t, w) = \frac{E[N(t, t+w)]}{w} \tag{4}$$

Not much can be said about the relationship between $\lambda(t)$ and $\nu(t, w)$ without knowing the exact probabilistic description of the point process. Nonetheless, the following statements, frequently explicitly (or implicitly) implemented in the neuroscientific studies [35–39] hold true:

1. Assume that the ISI sequence, $\{Y_1, Y_2, \dots\}$, forms a *renewal process*, i.e., a sequence of independent and identically distributed (i.i.d) random variables with probability density function (pdf),

$$Y \sim f_Y(y), \tag{5}$$

and mean ISI denoted as $E(Y)$. The renewal theorem [31] states that

$$\frac{1}{E(Y)} = \lim_{w\to\infty} \nu(t, w). \tag{6}$$

Note that Eq. (6) holds independently of t. In particular, it may therefore hold that $t = S_i$ or t is chosen randomly, without any reference to the point process realization. Moreover, Eq. (6) relates the mean firing rate to the mean ISI, and hence justifies the interpretation of $1/E(Y)$ as the mean *firing rate in the steady state* [4, 33].

2. Since the time origin is chosen without any reference to S_i, i.e., randomly with respect to the point process realization, the time of process observation, t, most likely falls within some particular ISI, say Y_k, and hence the time to first spike, $S_k - t$, generally does not follow the renewal pdf f_Y. The sequence of rvs $\{S_k - t, Y_{k+1}, Y_{k+2}, \dots\}$ is thus not stationary; however, the corresponding stochastic process is often denoted as a "steady state" or "equilibrium renewal" process, since $\lambda = \lambda(t)$ and $\nu(w) = \nu(t, w)$ do not depend on t anymore. The "firing rate/intensity" definitions above coincide and for all $w > 0$ it holds

$$\lambda = \frac{1}{E(Y)} = \nu(w). \tag{7}$$

2.2. Instantaneous interspike intervals and rate

Eqs. (6) and (7) show how the classical firing rate definitions based on spike counts and ISI averages are related to each other in the simple case of renewal firing. Consequently, Eq. (7) is potentially useful in determining the firing rate in steady-state situations only.

One of the first methods to deal with firing rate as a function of time was based on the concept of instantaneous firing rate [28, 29, 40–42], where the reciprocal values of ISIs are used to determine the firing rate (Fig. 1A)

$$X = \frac{1}{Y}. \tag{8}$$

There are several key differences between the classical firing rate and the instantaneous firing rate although the physical dimension (units of Hertz, or action potentials (spikes) per second) are the same. The most important difference is that the expected value of the instantaneous rate is higher than the count-based firing rate [13]

$$E(X) \geq \lambda, \tag{9}$$

with equality for perfectly regular neuronal firing (pacemaker) only.

Recently, Kostal *et al.* [30] showed that the incompatibility given by Eq. (9) is in fact naturally removed by noting that the value of X is *length-biased*. In other words, by observing the value of instantaneous rate at a given time t, we tend to observe longer ISIs with higher probability – denoted as the *instantaneous ISIs*. Consequently, for a renewal process of ISIs the value of X at time t follows the pdf,

$$X \sim f_X(x) = \frac{\lambda f_Y(1/x)}{x^3}, \tag{10}$$

which implies the desired result,

$$E(X) = \lambda. \tag{11}$$

See Kostal *et al.* [30] for details.

2.3. Kernel-based firing rate estimation

Several methods are commonly used to estimate neuronal firing rates from recorded neural data. These methods vary in complexity, computational requirements, and assumptions about the underlying neuronal processes, see Tomar [27] for a recent review.

For the purpose of comparison in this paper we choose the standard kernel-based firing rate estimation, which is a non-parametric method that estimates firing rate, $\hat{\lambda}(t)$, by convolving spike trains with a certain kernel function, $k_h(t)$,

$$\hat{\lambda}(t) = \sum_{i=1}^{n} k_h(t - s_i), \tag{12}$$

where $\{s_i\}_1^N$ are the time instants of individual spikes (i.e., realizations of r.v. S_i in Fig. 1A) in a spike train consisting of n spikes. For multiple spike trains the $\hat{\lambda}(t)$ is typically calculated by first pooling individual spike trains into a single resulting spike train on which the method for binwidth selection is applied [23].

The kernel-based approach provides a smooth estimate of firing rates and is less sensitive to the choice of bin size compared to histogram-based methods [11]. The kernel function typically depends on a smoothing parameter (also denoted as bandwidth), h. The value of h is either set *a priori* by the experimenter, or it is *optimized* in more advanced methods [22, 23, 25, 43], either globally or locally, in order to capture enough detail in the neuronal response. In addition, the kernel function satisfies the

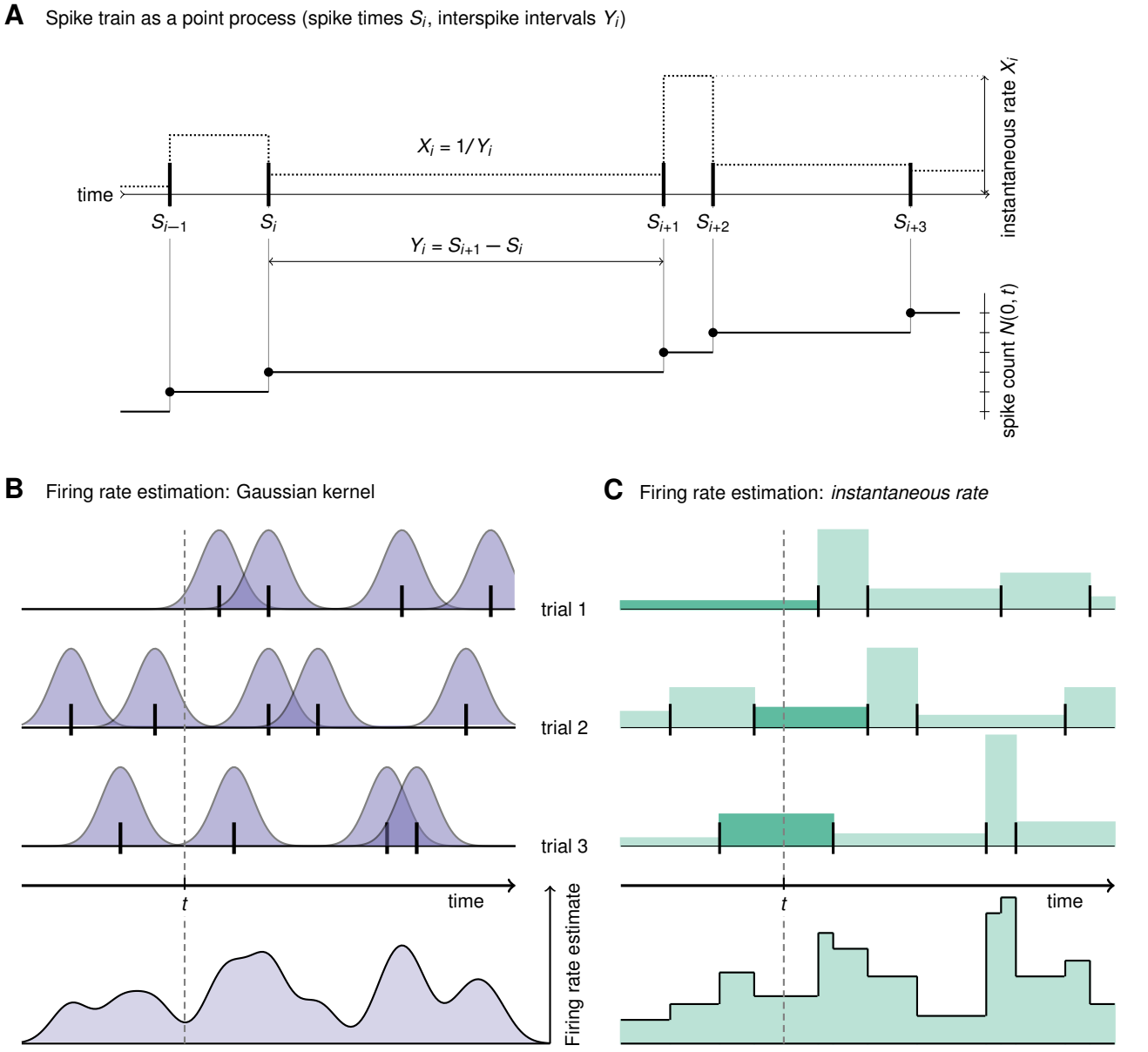

Figure 1. Graphical summary: Neuronal spiking activity as a stochastic point process and firing rate estimation. (**A**) Neuronal action potentials (spikes) occur at times S_i which are stochastic in general. The corresponding interspike intervals (ISI) are denoted as Y_i and the *instantaneous firing rate*, X_i, is a piecewise-constant function defined by the inverted value of the ISI length (dotted). The associated counting process $N(0,t)$ is needed for the general definition of the firing intensity (rate) $\lambda(t)$ (Eq. 3). (**B**) The classical *kernel-based* firing rate estimation is illustrated for the case of a Gaussian function. Each spike is replaced by a normal probability density function of mean zero and a certain variance (given by the binwidth, h, Eq. 16) and the firing rate estimate is a linear superposition of these Gaussian functions. In advanced estimation methods the binwidth is optimized locally to account for as much temporal detail as possible while providing a smoothed-out estimate of the firing rate. (**C**) The firing rate estimation introduced in this paper is based on the instantaneous rate of each individual trial (spike train). The value of the estimated firing rate at time t is generally a function of the instantaneous rate of each trial – either a simple average or a more complicated function as detailed in the Results section. In any case, the estimate is a piecewise-constant function with a point of change at each spike time. This method to some degree blurs the distinction between the *rate* and *temporal* coding schemes.

natural conditions [25]

$$k_h(t) \geq 0, \tag{13}$$

$$\int_{-\infty}^{\infty} k_h(t)\, dt = 1, \tag{14}$$

$$\int_{-\infty}^{\infty} t k_h(t)\, dt = 0. \tag{15}$$

For sufficiently dense spike trains the particular choice of kernel is of lesser importance than the bandwidth [25] and usually the Gaussian function is chosen (Fig. 1B),

$$k_h(t) = \frac{1}{\sqrt{2\pi} h(t)} \exp\left(-\frac{t^2}{2h(t)^2} \right). \tag{16}$$

Here we explicitly denote the possibility of bandwidth dependence on time.

In this paper, for the sake of comparison, we employ the (locally) optimized, i.e., time-dependent $h(t)$, according to the two following approaches:

i) Method of Shimazaki and Shinomoto [23]: building upon the technique they proposed before [44], the authors calculate the optimized bandwidth by minimizing a cost function involving the *mean integrated square error* (MISE) between the estimated rate and the unknown underlying rate. For the locally-optimal bandwidth the method divides the trial duration into local sub-intervals where the variable bandwidth is used. A local MISE function a is implemented in the local cost function to find the optimal bandwidth in the time window. There is an additional parameter to trade off the smoothness factor between the window length and optimal bandwidth. The resulting algorithm is computationally quite demanding for large datasets. The authors compare the fixed and variable kernel methods to the other established methods with sample spike data and confirm that the variable kernel estimation is more efficient in capturing the abrupt changes in the rate.

ii) Bayesian adaptive kernel smoothing (BAKS): Ahmadi *et al.* [22] employ simulated spike trains described by inhomogeneous Gamma and inhomogeneous inverse Gaussian processes to represent non-stationary neuronal firing. BAKS uses the kernel smoothing technique with adaptive bandwidth at the estimation points. The adaptive bandwidth is a random variable with prior distribution which is updated under a Bayesian framework given the spiking data. For the purpose of derivation, since the ISIs are modeled by Gamma distribution, the authors propose Gamma prior distribution on the precision parameter, which can be transformed into the variable bandwidth, and results into an analytical expression for the posterior. Consequently a closed-form expression for the bandwidth, in dependence on the spike times, is given. The authors compare BAKS to optimized kernel smoothing, variable kernel smoothing other estimation approaches. They report that BAKS compares favorably in terms of mean squared integrated error when tested on differing number of trials and different underlying rate functions. The advantage of BAKS, as opposed to the other Bayesian methods, is its lower computational complexity, and also when compared to Shimazaki and Shinomoto [23].

For further details on the methods and their implementation see Ahmadi *et al.* [22], Shimazaki and Shinomoto [23].

2.4. Cramér-Rao bound

The Eq. (11) binds the mean of the instantaneous firing rate to the firing rate, λ, of the renewal ISI process. It is natural then to ask how well can we *estimate* the true value of λ from the observed value $X = x$.

The problem of estimation precision, i.e., the evaluation of the smallest achievable error, is generally non-trivial [45, 46]. Instead, it is often more practical to evaluate the Cramér-Rao lower bound on the mean square error (MSE), of the estimator $\hat{\lambda}$,

$$\mathrm{MSE}(\hat{\lambda}) = E\big[(\hat{\lambda} - \lambda)^2\big]. \tag{17}$$

Under mild regularity conditions [47, 48], the Cramér-Rao bound states that the MSE of *any* estimator $\hat{\lambda}$ satisfies

$$\mathrm{MSE}(\hat{\lambda}) \geq \frac{1}{nJ(\lambda)}, \tag{18}$$

where n is the number of observations (sample size) used to evaluate $\hat{\lambda}$. The function $J(\lambda)$ is the *Fisher information*,

$$J(\lambda) = \int \left(\frac{\partial \log f_X(x;\lambda)}{\partial \lambda} \right)^2 f_X(x;\lambda)\, \mathrm{d}r, \tag{19}$$

where we explicitly denote the dependence of the p.d.f. of X on the firing rate λ, see Eq. (10).

The estimator efficiency, $\varepsilon(\hat{\lambda})$, is evaluated by using the Cramér-Rao bound from Eq. (18), i.e., by examining the ratio of the reciprocal value of the Fisher information against MSE in the limit of increasing n – thus often denoted as the *asymptotic* efficiency. More precisely,

$$\varepsilon(\hat{\lambda}_m) = \frac{1}{J(\lambda)} \frac{1}{\lim\limits_{n\to\infty} n\,\mathrm{MSE}(\hat{\lambda})}, \tag{20}$$

and it generally holds $\varepsilon(\hat{\lambda}_m) \leq 1$. If the ratio equals 1 then the estimator is *efficient* in the ultimate sense of the Cramér-Rao bound [49].

2.5. Renewal ISI models

In this section we briefly summarize several standard models of renewal neuronal firing which are completely

described by their pdf of ISIs. In the results section we employ the form of $f_Y(y;\lambda)$ in conjunction with Eq. (10) in order to derive maximum likelihood estimator of λ and to judge its (asymptotic) efficiency by means of Fisher information, Eq. (19).

Poisson neuron. The response spike-count distribution in many neurons is reported to be close to Poisson [34, 50, 51], especially if the firing intensity is approximately below 40 spikes/s [52]. Above that level the effect of maximum physiological firing rate (i.e., the refractory period – see below) becomes apparent. In the renewal, homogeneous case, the pdf of ISIs is given by the exponential,

$$f_Y(y;\lambda) = \lambda e^{-\lambda y}. \tag{21}$$

Poisson-like neuron with an absolute refractory period. The absolute refractory period is the time interval after every spike during which it is impossible for another spike to be emitted [1, 34]. The exponential pdf in Eq. (21) can be modified to account for the refractory period $\tau > 0$ as

$$f_Y(y;\lambda) = \begin{cases} a(\lambda)e^{-a(\lambda)(y-\tau)}, & \text{if } y > \tau, \\ 0, & \text{elsewhere,} \end{cases} \tag{22}$$

$$a(\lambda) = \frac{\lambda}{1-\lambda\tau}, \quad \lambda < 1/\tau. \tag{23}$$

As $\lambda \to 1/\tau$ the firing is described by a perfect pacemaker.

Gamma distribution. Due to its flexibility in shape, which accounts for all possible values of the ISI coefficient of variation C_V, and due to its close relationship to the exponential pdf (Poisson process), the gamma pdf is one of the most frequent statistical descriptors of ISIs employed in both experimental data analysis and theoretical considerations [22, 53–56]. The pdf parameterized by the ISI C_V is

$$f_Y(y;\lambda) = \left(\frac{\lambda}{C_V^2}\right)^{1/C_V^2} \Gamma(1/C_V^2)\, y^{1/C_V^2-1} \exp\left(-\frac{\lambda y}{C_V^2}\right), \tag{24}$$

where $C_V = \lambda\sqrt{\mathrm{Var}(Y)}$ and $\Gamma(z) = \int_0^\infty t^{z-1}\exp(-t)\,\mathrm{d}t$ is the gamma function [57].

Inverse Gaussian distribution. The renewal ISIs of the stochastic variant of the perfect integrate-and-fire neuronal model is described by the inverse Gaussian [34, 58]. In addition, the distribution is often fitted to experimental data as well [53, 59–61]. The pdf can be expressed in terms of ISI C_V as [62]

$$f_Y(y;\lambda) = \sqrt{\frac{1}{2\pi\lambda C_V^2 y^3}} \exp\left[-\frac{\lambda}{2C_V^2}\frac{(y-1/\lambda)^2}{y}\right]. \tag{25}$$

The lognormal distribution. With a handful of exceptions [63], lognormal pdf of ISIs is rarely presented as a result of a neuronal model. However, it represents quite a common descriptor in experimental data analysis [53, 61]. The pdf can be expressed as [62]

$$f_Y(y;\lambda) = \frac{1}{y\sqrt{2\pi\beta}} \exp\left\{-\frac{1}{8}\frac{[\beta + 2\log(y\lambda)]^2}{\beta}\right\}, \tag{26}$$

$$\beta = \log(1 + C_V^2). \tag{27}$$

3. RESULTS

Our main aim is to use Eq. (10) to derive the estimator of the firing rate λ. While Eq. (10) holds for the renewal case, in the strict sense, it is necessary to keep in mind that the value of instantaneous rate X, at time t, is given only by the ISI that *contains* the time t (see Fig. 1A, C and Kostal *et al.* [30]). The estimators derived below are therefore directly applicable to situations in which the instantaneous rate 'around' the time t follows the pdf $f_X(x)$. I.e., the proposed estimators are naturally applicable also to inhomogeneous, time-dependent cases as well. The proposed estimators, $\hat{\lambda}(t)$, are generally piecewise-constant functions with points of change occurring at spike times. Consequently, $\hat{\lambda}(t)$ behaves as a locally-adaptive 'bandwidth' estimator (using the kernel-based estimator terminology), where higher firing rates result in more temporal detail due to the accumulation of points of change (Fig. 1C).

3.1. Moment estimation of firing rate from the instantaneous rate

The Eq. (11) allows immediate estimation of the firing rate λ from a sample of of instantaneous rate values, independently from the particular ISI renewal model, f_Y.

Assume we have n trials (see Fig. 1C) so that at the time t we observe n instantaneous rate samples, $\{x_1, x_2, \ldots, x_n\}$. The moment estimator $\hat{\lambda}_m$ of λ is simply the average,

$$\hat{\lambda}_\mathrm{m} = \frac{1}{n}\sum_{i=1}^{n} x_i \tag{28}$$

The estimator can be viewed as a function of i.i.d. random variables X_i and therefore is a random variable itself.

In order to analyze the MSE of $\hat{\lambda}_m$, given by Eq. (17), we first note that the following relationship holds between the moments of instantaneous rate, X, and the interspike intervals, Y,

$$\mathrm{Var}(X) = E(X^2) - E(X)^2 = \frac{E(1/Y)}{E(Y)} - \frac{1}{E(Y)^2}, \tag{29}$$

which follows from Eq. (10) and due to Eq. (7) we have $\lambda = 1/E(Y)$. The behavior of $\mathrm{Var}(X)$ thus critically depends on $E(1/Y)$, which was also analyzed in Lansky *et al.* [13]. Due to Eqs. (11) and (28) the moment estimator is generally unbiased for all values of n,

$$E(\hat{\lambda}_\mathrm{m}) = \lambda, \tag{30}$$

while the MSE decreases with n as

$$\mathrm{MSE}(\hat{\lambda}_\mathrm{m}) = \frac{\lambda E(1/Y) - \lambda^2}{n}. \tag{31}$$

The Fisher information given by Eq. (19) has already been evaluated in Kostal *et al.* [30] in a closed form for the ISI renewal models $f_Y(y;\lambda)$ presented above. In particular, for the Poisson neuronal model we have $E(1/Y) = \infty$ and $J(\lambda) = 2/\lambda^2$, which makes the moment estimator not only inefficient, $\varepsilon(\hat{\lambda}_m) = 0$, but also not applicable in classical statistical scenarios. Once the refractory period is present, $E(1/Y)$ becomes finite [13], however it still holds $\varepsilon(\hat{\lambda}_m) < 1$ (calculation is very tedious and hence omitted). For the gamma pdf we have by the direct calculation of $\mathrm{Var}(X)$ and from Kostal *et al.* [30],

$$J(\lambda) = \frac{1 + C_V^2}{\lambda^2}, \tag{32}$$

$$\mathrm{MSE}(\hat{\lambda}_m) = \frac{1}{n}\frac{C_V^2\lambda^2}{1 - C_V^2}, \quad \text{for } C_V < 1, \tag{33}$$

therefore the estimator monotonically approaches the efficient regime, $\varepsilon(\hat{\lambda}_m) = 1$, as $C_V \to 0$. For both the inverse Gaussian and lognormal ISI renewal models we have $\lim_{n\to\infty} n\,\mathrm{MSE}(\hat{\lambda}_\mathrm{m}) = C_V^2\lambda^2$, while $J(\lambda) = (2 + C_V^2)/(2C_V^2\lambda^2)$ for the inverse Gaussian, and $J(\lambda) = 1/(\beta\lambda^2)$ for the lognormal. The estimators are thus not efficient.

3.2. Maximum-likelihood estimation of firing rate from the instantaneous rate

The moment estimator in Eq. (28) does not require the exact knowledge of $f_X(x)$, nonetheless the simplicity is counterbalanced by its inefficiency. On the other hand, the maximum-likelihood (ML) estimator, $\hat{\lambda}_\mathrm{ML}$,

$$\hat{\lambda}_\mathrm{ML} = \arg\max_\lambda \sum_{i=1}^{n} \log f_X(x_i;\lambda), \tag{34}$$

is asymptotically *efficient*, under mild technical assumptions [49], which are satisfied in the context of this paper. See Pilarski and Pokora [48] for a review of the conditions in the computational neuroscience context.

As the Eq. (34) suggests, it is difficult to obtain a closed-form expression for the estimator $\hat{\lambda}_\mathrm{ML}$, its mean and variance, or even its entire pdf for the renewal firing models of interest. Nonetheless, at least for the Poisson and gamma model it is possible to obtain the complete statistics of $\hat{\lambda}_\mathrm{ML}$, and also to derive a closed-form expression for the ML estimator for the Poisson neuron with refractory period.

Poisson neuron. First, we introduce the auxiliary random variable $Z = 1/X$, which is gamma-distributed with $E(Z) = 2/\lambda$, as follows from the standard transformation rule for probability density functions and [64] and Eq. (10),

$$Z \sim \lambda^2 z e^{-\lambda z}. \tag{35}$$

The sample mean divided by two, $\sum_i z_i/(2n)$, is therefore the ML estimator of the mean ISI, $E(Y) = 1/\lambda$, furthermore it is also unbiased and efficient [65]. Due to the invariance property of the ML estimator [65, p. 444] it holds

$$\hat{\lambda}_\mathrm{ML} = \left(\frac{1}{2n}\sum_{i=1}^{n}\frac{1}{x_i}\right)^{-1}. \tag{36}$$

Second, the sum $V = \sum_{i=1}^{n} 1/X_i$ follows the gamma pdf, $\gamma(v; 2n, \lambda)$,

$$\gamma(x;\alpha,\beta) = \frac{\beta^\alpha}{\Gamma(\alpha)}x^{\alpha-1}e^{-\beta x}, \tag{37}$$

with the shape parameter equal to $2n$ and the rate parameter equal to λ due to the summation property of i.i.d. gamma-distributed random variables with equal rate parameter [66]. Applying the transformation $\hat{\lambda}_\mathrm{ML} = (2nV)^{-1}$ on $V \sim \gamma(v; 2n, \lambda)$ yields the complete pdf of the ML estimator,

$$\hat{\lambda}_\mathrm{ML} \sim \frac{(2n\lambda)^{2n}}{\Gamma(2n)}(\hat{\lambda}_\mathrm{ML})^{-2n-1}\exp\left(-\frac{2n\lambda}{\hat{\lambda}_\mathrm{ML}}\right), \tag{38}$$

from which it follows

$$E(\hat{\lambda}_\mathrm{ML}) = \lambda\frac{2n}{2n-1}, \tag{39}$$

$$\mathrm{Var}(\hat{\lambda}_\mathrm{ML}) = \frac{(2n\lambda)^2}{(2n-1)^2(2n-2)}, \quad n \geq 2, \tag{40}$$

and hence

$$\begin{aligned}\mathrm{MSE}(\hat{\lambda}_\mathrm{ML}) &= \mathrm{Var}(\hat{\lambda}_\mathrm{ML}) + \left[E(\hat{\lambda}_\mathrm{ML}) - \lambda\right]^2 \\ &= \frac{(1+n)\lambda^2}{(n-1)(2n-1)}.\end{aligned} \tag{41}$$

Note that although the ML estimator is biased, $E(\hat{\lambda}_\mathrm{ML}) \neq \lambda$, the bias depends only on n and not on λ, so it is possible to un-bias the ML estimator and also to reduce its MSE by considering

$$\hat{\lambda}_\mathrm{MLU} = \left(\frac{1}{2n-1}\sum_{i=1}^{n}\frac{1}{r_i}\right)^{-1}, \tag{42}$$

which yields

$$E(\hat{\lambda}_\mathrm{MLU}) = \lambda, \tag{43}$$

$$\mathrm{MSE}(\hat{\lambda}_\mathrm{MLU}) = \frac{\lambda^2}{2n-2}, \quad n \geq 2. \tag{44}$$

The unbiased ML estimator is asymptotically efficient, since $\lim_{n\to\infty} n\,\mathrm{MSE}(\hat{\lambda}_\mathrm{MLU}) = 1/J(\lambda) = \lambda^2/2$.

Gamma distribution of ISIs. It is possible to extend the derivation of Eq. (42) to the case of ISIs following the gamma pdf in Eq. (24). Then Eq. (42) is a special case for $C_V = 1$.

Let the ISI pdf of Y be rewritten as $f_Y(y) = \gamma(y; C_V^{-2}, \lambda C_V^{-2})$ as in Eq. (37), since for $\gamma(z; \alpha, \beta)$ it holds $E(Z) = \alpha/\beta$ and $C_V = 1/\sqrt{\alpha}$. Therefore for the auxillary variable $Z = 1/X$ it holds

$$Z \sim \gamma(z; 1 + C_V^{-2}, \lambda C_V^{-2}), \tag{45}$$

due to Eq. (10) and the pdf transformation rule [64], and hence $E(Z) = (1+C_V^2)/\lambda$. The rest of the argument is the same as above. Namely, $\sum_i z_i/(\alpha n)$, where $\alpha = 1 + C_V^{-2}$, is the ML estimator of C_V^2/λ, i.e., $\sum_i z_i/[(1 + C_V^2)n]$ is the ML estimator of $1/\lambda$, and therefore

$$\hat{\lambda}_{\mathrm{ML}} = n(1 + C_V^2)\left(\sum_{i=1}^{n} \frac{1}{x_i}\right)^{-1} \tag{46}$$

is the ML estimator of λ.

The sum $V = \sum_{i=1}^{n} 1/X_i$ follows the gamma distribution, $\gamma\big(v; n(1 + C_V^{-2}), \lambda C_V^{-2}\big)$, hence the transformation $\hat{\lambda}_{\mathrm{ML}} = \big(n(1 + C_V^2)V\big)^{-1}$ applied to V yields the inverted gamma pdf [67], $\hat{\lambda}_{\mathrm{ML}} \sim \gamma_{\mathrm{inv}}\big(\hat{\lambda}_{\mathrm{ML}}; n(1 + C_V^{-2}), n\lambda(1 + C_V^{-2})\big)$, where

$$\gamma_{\mathrm{inv}}(x; \alpha, \beta) = \frac{\beta^\alpha}{\Gamma(\alpha)} x^{-\alpha-1} e^{-\beta/x}. \tag{47}$$

The mean of the estimator is biased,

$$E(\hat{\lambda}_{\mathrm{ML}}) = \lambda \frac{(1 + C_V^2)n}{(n-1)C_V^2 + n}. \tag{48}$$

The bias correction is possible and for the un-biased ML estimator we have (for $n \geq 2$),

$$\hat{\lambda}_{\mathrm{MLU}} = \big((n-1)C_V^2 + n\big)\left(\sum_{i=1}^{n} \frac{1}{x_i}\right)^{-1}, \tag{49}$$

$$E(\hat{\lambda}_{\mathrm{MLU}}) = \lambda, \tag{50}$$

$$\mathrm{MSE}(\hat{\lambda}_{\mathrm{MLU}}) = \frac{C_V^2 \lambda^2}{(n-2)C_V^2 + n}. \tag{51}$$

It is worth noting that $\mathrm{MSE}(\hat{\lambda}_{\mathrm{MLU}}) < \mathrm{MSE}(\hat{\lambda}_{\mathrm{ML}})$ for all $n \geq 2$, and that $\lim_{n\to\infty} n\,\mathrm{MSE}(\hat{\lambda}_{\mathrm{MLU}})$ also equals $1/J(\lambda)$, hence Eq. (49) is indeed the asymptotically efficient estimator of λ for all values of C_V. Also note that for $n = 1$ the estimator does not depend on C_V, and just equals x_1, as expected.

Mismatched estimation. It is possible to derive the mean and MSE of the *mismatched* estimation [49], that is, when $\hat{\lambda}_{\mathrm{MLU}}$ from Eq. (42) uses observations x_i resulting from the gamma ISI p.d.f. in Eq. (24). Such estimation is mismatched for all $C_V \neq 1$. The p.d.f. of the mismatched estimator follows $\gamma_{\mathrm{inv}}\big(\hat{\lambda}_{\mathrm{MLU}}; n(1 + C_V^2), n\lambda(1 + C_V^{-2})\big)$, and thus

$$E(\hat{\lambda}_{\mathrm{MLU}}) = \lambda \frac{2n - 1}{C_V^2(n-1) + n}. \tag{52}$$

It holds $\lim_{n\to\infty} \mathrm{Var}(\hat{\lambda}_{\mathrm{MLU}}) = 0$, and, asymptotically, the mismatched estimator is biased,

$$\lim_{n\to\infty} E(\hat{\lambda}_{\mathrm{MLU}}) - \lambda = \lambda \frac{1 - C_V^2}{1 + C_V^2}. \tag{53}$$

Poisson neuron with a refractory period. The presence of refractory period $\tau > 0$ in Eq. (22) makes it impossible to apply the method of transformations, which we employed to derive Eqs. (42) and (49). In fact, it seems analytically intractable to obtain the full pdf of the ML estimator in this case, however, it is possible to obtain a simple closed-form expression for the estimator itself. In order to derive the expression we substitute Eq. (22) directly into Eq. (34), and set the derivative of the log-likelihood function, $\ell(\lambda) = \sum_{i=1}^{n} \log f_X(x_i; \lambda)$, equal to zero in order to find the maximum.

The derivative of the log-likelihood function can be manipulated into the form

$$\frac{\mathrm{d}\ell(\lambda)}{\mathrm{d}\lambda} = \left(n + \frac{n - n\lambda\mu}{(\lambda\tau - 1)^2}\right)\frac{1}{\lambda}, \tag{54}$$

where $\mu = \sum_{i=1}^{n} (nx_i)^{-1}$. Equating the expression in Eq. (54) to zero yields the solution

$$\hat{\lambda}_{\mathrm{ML}} = \frac{\mu + 2\tau - \sqrt{\mu^2 + 4\mu\tau - 4\tau^2}}{2\tau^2}. \tag{55}$$

Due to the presence of the square root in Eq. (55) it is not possible to obtain the ML estimator mean and the MSE analytically.

3.3. Estimation of firing rate from simulated spike trains

Finally, we compare the newly derived estimators with state-of-art self-adaptive firing rate estimation methods by using simulated spike trains. In order to make the comparison of the proposed and traditional approaches both 'manageable' and comprehensible, we have to limit ourselves in the choice of the following categories: *i)* the neuronal firing models, *ii)* the classical firing rate estimators and *iii)* the newly proposed estimators.

i) Experimentally recorded neuronal firing is often well approximated by the Poisson process with refractory period [50–52, 68, 69]. Therefore we simulate neuronal activity as an inhomogeneous generalized Poisson process with firing intensity $\lambda(t)$ and refractory period τ. I.e., we use Eq. (23) to simulate a classical inhomogeneous Poisson process with the rescaled

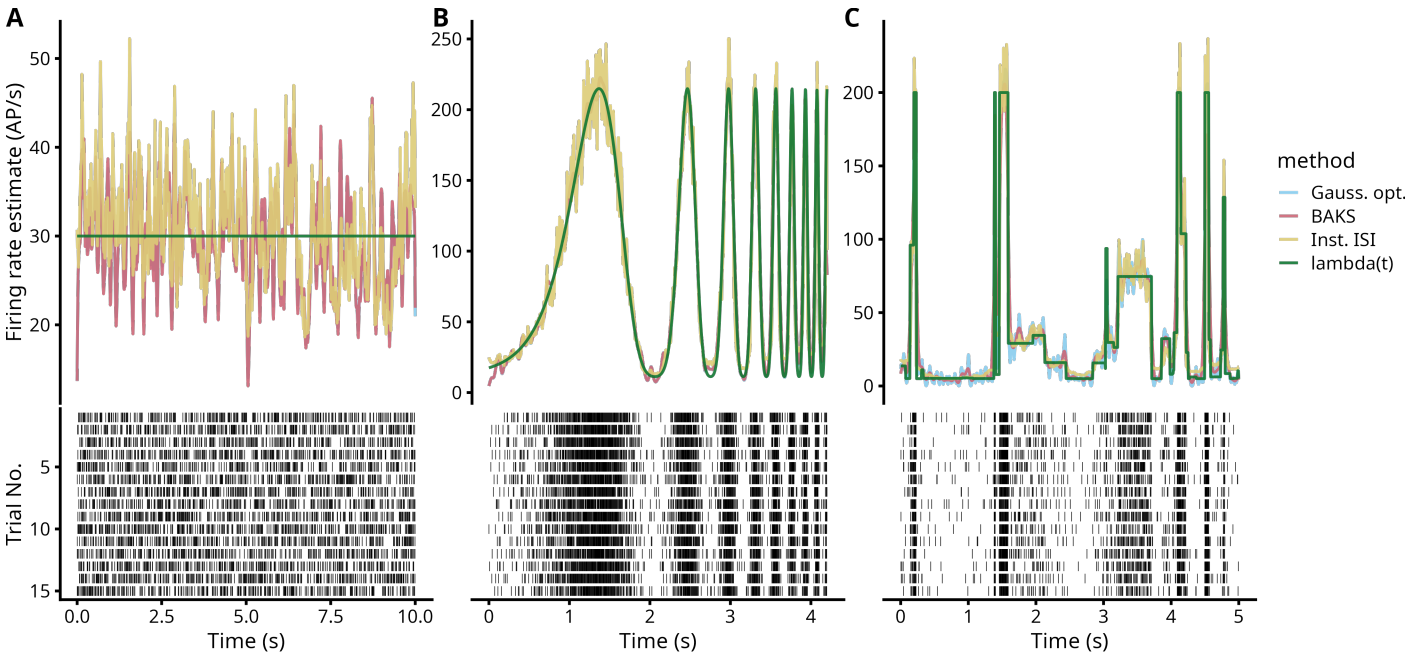

Figure 2. Comparison of firing rate estimators for simulated sets (trials) of 15 spike trains of duration 5 s. The spike trains follow the (inhomogeneous) Poisson process with refractory period $\tau = 3$ ms. Three firing rate functions $\lambda(t)$ are considered to cover distinct situations: (**A**) *constant*, 30 Hz steady-state firing rate, (**B**) *aperiodic*, to demonstrate the performance with slow-rapid but smooth firing rate changes, (**C**) *fluctuating*, mimicking the sudden discontinuous changes in firing rate (observed, e.g., in the insect olfactory receptory neurons). The respective spike trains are shown in the bottom panels. Two standard Gaussian kernel-based techniques (*Gauss. opt.* based on the adaptive estimator by Shimazaki and Shinomoto [23] and the locally adaptive Bayesian *BAKS* by Ahmadi *et al.* [22]) are shown in comparison with the novel estimator *Inst. ISI* based on Eq. (55). Unlike the two considered Gaussian estimators, the instantaneous firing rate estimator tends to capture rapid firing rate increase better (perhaps even overestimating it). On the other hand it is also more 'noisy' and does not follow the low-firing periods, especially in (C), too precisely (see the Discussion and Conclusions).

rate, $a[\lambda(t)]$, and then thin the resulting spike train with the refractory period. We employ the following three distinct time courses of $\lambda(t)$, The refractory period is set to $\tau = 3$ ms in all cases:

(a) *constant* (Fig. 2A), $\lambda(t) = 30$ Hz steady-state firing rate,

(b) *aperiodic* (Fig. 2B), progressively decreasing 'periodicity' as $\lambda(t) = (\cos[3\cos(2e^t/5)] + 1) \times 100$ Hz, to demonstrate the performance with slow-rapid but smooth firing rate changes, similar to the 'chirp' signal [22],

(c) *fluctuating* (Fig. 2C), mimicking the rapid discontinuous changes of firing rate as observed, e.g., in the insect olfactory receptory neurons [70, 71].

ii) For the sake of estimator performance analysis we choose the adaptive approaches, as detailed in the Methods section (Fig. 2),

(a) *Gauss. opt.*: by Shimazaki and Shinomoto [23],

(b) *BAKS*: by Ahmadi *et al.* [22].

iii) We believe that especially Eq. (55), despite lacking the detailed mean and MSE analysis, has a potential for practical utilization and therefore we choose it for the comparison. While the refractory period is known for the simulation purposes, we estimate it from the data as

$$\hat{\tau} = \min\{s_i\}, \tag{56}$$

where $\{s_i\}$ is the set of all ISIs in the data (e.g., in every spike train and every trial). We note that more advanced and unbiased statistical methods for the refractory period estimation exist in the literature [72], however, Eq. (56) is entirely sufficient for the testing purposes. This estimator is denoted as '*Inst. ISI*' in Figs. 2 and 3. Furthermore, we note our $\hat{\lambda}(t)$ can itself be used to determine the locally adaptive Gaussian kernel bandwidth (Eq. 16),

$$h(t) = \frac{c}{\hat{\lambda}(t)}, \tag{57}$$

where $\hat{\lambda}(t)$ is given, e.g., by Eq. (55) and c is a suitable constant. We did not optimize for c and set it by hand to $c = 1/2$ instead. This estimator is denoted as '*Inst. ISI: local*' in Fig. 3.

The relative (i.e., divided by the 'average' $\lambda(t)$ squared) mean integrated square error (MISE) is selected as the

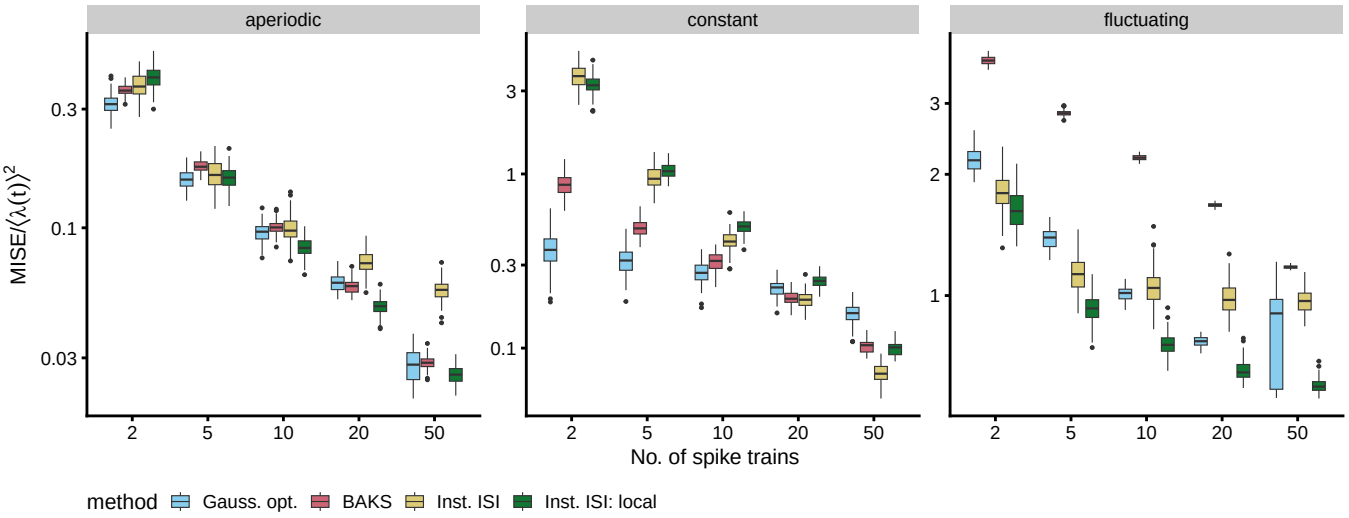

Figure 3. Comparison of firing rate estimators for the three distinct cases of firing rate functions, $\lambda(t)$, shown in Fig 2: the *aperiodic* (Fig 2B), the *constant* (Fig 2A) and the *fluctuating* (Fig 2C). The comparison shows the *relative* MISE (Eq. 58) in dependence on the number of parallelly simulated spike trains (Fig. 1C). The estimation methods correspond to Fig 2, with the addition of the '*Inst. ISI: local*' method, whereby the reciprocal value of $\hat{\lambda}_{\mathrm{MLU}}$ is used to determine the locally-adaptive Gaussian kernel bandwidth (Eq. 57). The results are based on 200 repetitions. In most cases we observe the superior performance of the method proposed by Shimazaki and Shinomoto [23] though the computational cost is an issue. There are exceptions in terms of both the sample size and the $\lambda(t)$ shape. It is not suprising that with an increasing sample size the Eq. (55) (Inst. ISI) overperforms the other methods due to its maximum-likelihood derivation. In the case of a rapidly fluctuating firing rate Eq. (57) seems to be superior to the other approaches – unlike the case of the *constant* $\lambda(t)$.

performance indicator and evaluated numerically (Fig. 3),

$$\frac{\mathrm{MISE}}{\langle\lambda(t)\rangle^2} = \frac{\int \left[\hat{\lambda}(t) - \lambda(t)\right]^2 \mathrm{d}t}{\left[\int \lambda(t)\,\mathrm{d}t\right]^2}. \tag{58}$$

4. DISCUSSION AND CONCLUSIONS

Fig. 2 shows the firing rate estimators, under the conditions described above, for 15 simulated spike trains of duration 5 s each. We see that the instantaneous firing rate estimator based on Eq. (55) tends to capture the rapid firing rate fluctuations better than the optimized kernel-based estimators. On the other hand it is also more noisy and does not follow the low-firing periods precisely, especially in Fig. 2C. The explanation lies in the fact that although we formally require $\lambda(t) > 0$ at all times [73], the largest instantaneous ISI is determined by the time interval between two spikes. In other words, in the inhomogeneous situation, whenever we have a high-intensity firing separated by a short gap of low firing (almost zero intensity), the value of X is effectively lower-bounded by the 'gap' duration. This observation leads us to propose Eq. (57)

Fig. 3 compares the firing rate estimators for the three distinct cases of firing rate functions. The comparison shows the relative MISE given by (Eq. 58) in dependence on the number of simulated spike trains (Fig. 1C). The state-of-art method proposed by Shimazaki and Shinomoto [23] provides very good results, however, the computational cost is an issue – the locally-adaptive approach is a nested optimization problem, making its implementation numerically prohibitive for large data sets. It is not surprising that with an increasing sample size the Eq. (55) (Inst. ISI) overperforms the other methods due to its maximum-likelihood derivation. On the other hand, Eq. (57) seems to be superior to the other approaches in case of a rapidly fluctuating driving intensity – and its computational cost is negligible.

We conclude the paper with the following observations:

i) The moment estimators based on the instantaneous rate are not efficient and perform rather poorly with increasing C_V. Such behavior can be expected intuitively, as spike bursts can influence $\hat{\lambda}$ significantly.

ii) The newly derived estimators in Eqs. (42), (49) and (55) are computationally very simple to apply, even for very large datasets, and *free* of additional parameters which would require further optimization.

iii) The estimators in Eqs. (42), (49) and (55) are essentially 'locally adaptive' or 'local', i.e., the time scale on which the estimated intensity changes is given by the ISIs themselves (see Fig. 1C). The higher the firing rate – the more detail. Typically, the advanced adaptive estimation methods require whole spike trains to be known first (in order to optimize the bandwidth), the new estimator adapts 'on-line',

may be applied to any small segment of the whole record.

iv) The ISIs from individual trials are generally not pooled (as compared with classical kernel-based estimators).

v) The algebraic simplicity of Eq. (55) makes it a good candidate for the universal estimator of $\lambda(t)$ even in situations when the likelihood function is not known exactly or when solving Eq. (34) is intractable. This is further supported by the fact that neuronal firing is often close to the Poissonian regime.

---

[1] W. Gerstner and W. M. Kistler, *Spiking Neuron Models: Single Neurons, Populations, Plasticity* (Cambridge University Press, Cambridge, 2002).

[2] M. N. Shadlen and W. T. Newsome, "The variable discharge of cortical neurons: Implications for connectivity, computation, and information coding," J. Neurosci. **18**, 3870–3896 (1998).

[3] R. B. Stein, E. R. Gossen, and K. E. Jones, "Neuronal variability: noise or part of the signal?" Nat. Rev. Neurosci. **6**, 389–397 (2005).

[4] L. Kostal, P. Lansky, and J-P. Rospars, "Review: neuronal coding and spiking randomness," Eur. J. Neurosci. **26**, 2693–2701 (2007).

[5] P. Dayan and L. F. Abbott, *Theoretical Neuroscience: Computational and Mathematical Modeling of Neural Systems* (MIT Press, Cambridge, 2001).

[6] E. D. Adrian, *Basis of Sensation* (W. W. Norton and Co., New York, 1928).

[7] E. R. Kandel, J. H. Schwartz, and T. M. Jessel, *Principles of neural science* (Elsevier, New York, 1991).

[8] H. Lee, L. Kostal, R. Kanzaki, and R. Kobayashi, "Spike frequency adaptation facilitates the encoding of input gradient in insect olfactory projection neurons," Biosystems **223**, 104802 (2023).

[9] L. Kostal and R. Kobayashi, "Critical size of neural population for reliable information transmission," Phys. Rev. E (Rapid Commun.) **100**, 050401(R) (2019).

[10] M. Abeles, "Firing rates and well-timed events in the cerebral cortex," in *Models of Neural Networks II*, edited by E. Domany, K. Schulten, and J. L. van Hemmen (Springer, New York, 1994) pp. 121–138.

[11] S. Shinomoto, "Estimating the firing rate," in *Analysis of parallel spike trains*, edited by S. Grün and S. Rotter (Springer, Boston, MA, 2010) pp. 21–35.

[12] S. Koyama and L. Kostal, "The effect of interspike interval statistics on the information gain under the rate coding hypothesis," Math. Biosci. Eng. **11**, 63–80 (2014).

[13] P. Lansky, R. Rodriguez, and L. Sacerdote, "Mean instantaneous firing frequency is always higher than the firing rate," Neural Comput. **16**, 477–489 (2004).

[14] M. N. Shadlen and W. T. Newsome, "Noise, neural codes and cortical organization," Curr. Opin. Neurobiol. **4**, 569–579 (1994).

[15] R. Kobayashi and K. Kitano, "Impact of slow K^+ currents on spike generation can be described by an adaptive threshold model," J. Comput. Neurosci. **40**, 347–362 (2016).

[16] M. S. Fuller and F. J. Looft, "An information-theoretic analysis of cutaneous receptor responses," IEEE Trans. Biomed. Eng. **31**, 377–383 (1984).

[17] J. C. Middlebrooks, A. E. Clock, L. Xu, and D. M. Green, "A panoramic code for sound location by cortical neurons," Science **264**, 842–844 (1994).

[18] D. H. Perkel and T. H. Bullock, "Neural coding," Neurosci. Res. Prog. Sum. **3**, 405–527 (1968).

[19] F. Rieke, R.R. de Ruyter van Steveninck, D. Warland, and W. Bialek, *Spikes: Exploring the Neural Code* (MIT Press, Cambridge, 1997).

[20] F. Theunissen and J. P. Miller, "Temporal encoding in nervous systems: A rigorous definition," J. Comput. Neurosci. **2**, 149–162 (1995).

[21] L. Kostal and R. Kobayashi, "Optimal decoding and information transmission in Hodgkin-Huxley neurons under metabolic cost constraints," BioSystems **136**, 3–10 (2015).

[22] N. Ahmadi, T. G. Constandinou, and C-S. Bouganis, "Estimation of neuronal firing rate using Bayesian Adaptive Kernel Smoother (BAKS)," PLoS ONE **13**, e0206794 (2018).

[23] H. Shimazaki and S. Shinomoto, "Kernel bandwidth optimization in spike rate estimation," J. Comput. Neurosci. **29**, 171–182 (2010).

[24] E. Benedetto, F. Polito, and L. Sacerdote, "On firing rate estimation for dependent interspike intervals," Neural Comput. **27**, 699–724 (2015).

[25] M. Nawrot, A. Aertsen, and S. Rotter, "Single-trial estimation of neuronal firing rates: from single-neuron spike trains to population activity," J. Neurosci. Meth. **94**, 81–92 (1999).

[26] S. Koyama and S. Shinomoto, "Histogram bin width selection for time-dependent Poisson processes," J. Phys. A: Math. Gen. **37**, 7255–7265 (2004).

[27] R. Tomar, "Review: Methods of firing rate estimation," Biosystems **183**, 103980 (2019).

[28] P. Bessou, Y. Laporte, and B. Pagés, "A method of analysing the responses of spindle primary endings to fusimotor stimulation," J. Physiol. **196**, 37–75 (1968).

[29] B. W. Knight, "The relationship between the firing rate of a single neuron and the level of activity in a population of neurons," J. Gen. Physiol. **59**, 767–778 (1972).

[30] L. Kostal, P. Lansky, and M. Stiber, "Statistics of inverse interspike intervals: the instantaneous firing rate revisited," Chaos **28**, 106305 (2018).

[31] D. R. Cox and P. A. W. Lewis, *The statistical analysis of series of events* (Latimer Trend and Co. Ltd., Whistable, 1966).

[32] R. E. Kass, V. Ventura, and E. N. Brown, "Statistical issues in the analysis of neuronal data," J. Neurophysiol. **94**, 8–25 (2005).

[33] G. P. Moore, D. H. Perkel, and J. P. Segundo, "Statistical analysis and functional interpretation of neuronal spike data," Annu. Rev. Physiol. **28**, 493–522 (1966).

[34] H. C. Tuckwell, *Introduction to Theoretical Neurobiology,*

Vol. 2 (Cambridge University Press, New York, 1988).
[35] W. Braun, R. Thul, and A. Longtin, "Evolution of moments and correlations in nonrenewal escape-time processes," Phys. Rev. E **95**, 052127 (2017).
[36] J. Doose and B. Lindner, "Evoking prescribed spike times in stochastic neurons," Phys. Rev. E **96**, 032109 (2017).
[37] G. D'Onofrio, P. Lansky, and E. Pirozzi, "On two diffusion neuronal models with multiplicative noise: The mean first-passage time properties," Chaos **28**, 043103 (2018).
[38] A. Peterson and P. Heil, "A simple model of the inner-hair-cell ribbon synapse accounts for mammalian auditory-nerve-fiber spontaneous spike times," Hearing Res. **363**, 1–27 (2018).
[39] M. Tamborrino, "Approximation of the first passage time density of a Wiener process to an exponentially decaying threshold by two-piecewise linear threshold. Application to neuronal spiking activity," Math. Biosci. Eng. **13**, 613–629 (2016).
[40] A. Sawczuk, R. K. Powers, and M. D. Binder, "Spike frequency adaptation studied in hypoglossal motoneurons of the rat," J. Neurophysiol. **73**, 1799–1810 (1995).
[41] S. Martinez-Conde, S. L. Macknik, and D. H. Hubel, "Microsaccadic eye movements and firing of single cells in the striate cortex of macaque monkeys," Nature **3**, 251–258 (2000).
[42] J-P. Rospars, P. Lansky, A. Duchamp, and P. Duchamp-Viret, "Relation between stimulus and response in frog olfactory receptor neurons *in vivo*," Eur. J. Neurosci. **18**, 1135–1154 (2003).
[43] D. O. Loftsgaarden and C. P. Quesenberry, "A nonparametric estimate of a multivariate density function," Ann. Math. Stat **36**, 1049–1051 (1965).
[44] H. Shimazaki and S. Shinomoto, "A method for selecting the bin size of a time histogram," Neural Comput. **19**, 1503–1527 (2007).
[45] H. L. van Trees and K. L. Bell, *Detection, Estimation and Modulation Theory, Part I* (John Wiley and Sons, New York, 2013).
[46] L. Kostal, P. Lansky, and S. Pilarski, "Performance breakdown in optimal stimulus decoding," J. Neural Eng. **12**, 036012 (2015).
[47] L. A. Ibragimov and R. Z. Has'minskii, *Statistical Estimation – Asymptotic Theory* (Springer-Verlag, New York, 1981).
[48] S. Pilarski and O. Pokora, "On the Cramér-Rao bound applicability and the role of Fisher information in computational neuroscience," BioSystems **136**, 11–22 (2015).
[49] A. W. van der Vaart, *Asymptotic statistics* (Cambridge University Press, Cambridge, UK, 2000).
[50] M. C. Teich and S. M. Khanna, "Pulse-number distribution for the neural spike train in the cat's auditory nerve," J. Acoustic. Soc. Am. **77**, 1110–1128 (1985).
[51] R. L. Winslow and M. B. Sachs, "Single-tone intensity discrimination based on auditory-nerve rate responses in background of quiet, noise, and with stimulation of the crossed olivocochlear bundle," Hearing Res. **35**, 165–190 (1988).
[52] E. Javel and N. F. Viemeister, "Stochastic properties of cat auditory nerve responses to electric and acoustic stimuli and application to intensity discrimination," J. Acoust. Soc. Am. **107**, 908–921 (2000).
[53] M. W. Levine, "The distribution of the intervals between neural impulses in the maintained discharges of retinal ganglion cells," Biol. Cybern. **65**, 459–467 (1991).
[54] D. E. McKeegan, "Spontaneous and odour evoked activity in single avian olfactory bulb neurones," Brain Res. **929**, 48–58 (2002).
[55] K. Rajdl and L. Kostal, "Estimation of the instantaneous spike train variability," Chaos Solit. Fractals **177**, 114280 (2023).
[56] K. Rajdl, P. Lansky, and L. Kostal, "Entropy factor for randomness quantification in neuronal data," Neural Netw. **95**, 57–65 (2017).
[57] M. Abramowitz and I. A. Stegun, *Handbook of Mathematical Functions, With Formulas, Graphs, and Mathematical Tables* (Dover, New York, 1965).
[58] P. Lansky and S. Sato, "The stochastic diffusion models of nerve membrane depolarization and interspike interval generation." J. Peripher. Nerv. Syst. **4**, 27–42 (1999).
[59] D. Berger, K. Pribram, H. Wild, and C. Bridges, "An analysis of neural spike-train distributions: determinants of the response of visual cortex neurons to changes in orientation and spatial frequency," Exp. Brain Res. **80**, 129–134 (1990).
[60] G. L. Gerstein and B. Mandelbrot, "Random walk models for the spike activity of a single neuron," Biophys. J. **4**, 41–68 (1964).
[61] C. Pouzat and A. Chaffiol, "Automatic Spike Train Analysis and Report Generation. An Implementation with R, R2HTML and STAR," J. Neurosci. Methods **181**, 119–144 (2009).
[62] L. Kostal and P. Lansky, "Variability and randomness in stationary neuronal activity," BioSystems **89**, 44–49 (2007).
[63] A. Bershadskii, E. Dremencov, D. Fukayama, and G. Yadid, "Probabilistic properties of neuron spiking time-series obtained in vivo," Eur. Phys. J. B **24**, 409–413 (2001).
[64] A. Papoulis, *Probability, random variables, and stochastic processes* (McGraw-Hill, New York, 1991).
[65] E. L. Lehmann and G. Casella, *Theory of point estimation* (Springer Verlag, New York, 1998).
[66] N. Johnson, S. Kotz, and N. Balakrishnan, *Continuous Univariate Distributions, Vol. 1* (John Wiley & Sons, New York, 1994).
[67] V. Witkovsky, "Computing the distribution of a linear combination of inverted gamma variables," Kybernetika **37**, 79–90 (2001).
[68] M. Abeles, *Local cortical circuits: Studies of brain function*, Vol. 6 (Springer-Verlag, Berlin, 1982).
[69] S. Deneve, "Bayesian spiking neurons I: inference," Neural Comput. **20**, 91–117 (2008).
[70] M. Levakova, L. Kostal, C. Monsempès, V. Jacob, and P. Lucas, "Moth olfactory receptor neurons adjust their encoding efficiency to temporal statistics of pheromone fluctuations," PLoS Comput. Biol. **14**, e1006586 (2018).
[71] M. Levakova, L. Kostal, C. Monsempès, P. Lucas, and R. Kobayashi, "Adaptive integrate-and-fire model reproduces the dynamics of olfactory receptor neuron responses in moth," J. R. Soc. Interface **16**, 20190246 (2019).
[72] D. Hampel and P. Lansky, "On the estimation of refractory period," J. Neurosci. Meth. **171**, 288–295 (2008).
[73] D. J. Daley and D. Vere-Jones, *An Introduction to the Theory of Point Processes, Vol. I* (Springer, New York, USA, 2002).